

Repair Abilities of Mouse Autologous Adipose-Derived Stem Cells and ShakeGel™3D Complex Local Injection With Intrauterine Adhesion by BMP7-Smad5 Signaling Pathway Activation

Yun-xia Zhao (✉ 15983781153@163.com)

Second Affiliated Hospital of Fujian Medical University <https://orcid.org/0000-0002-0195-5031>

Qiao-yi Huang

Second Affiliated Hospital of Fujian Medical University

Wei-can Chen

Second Affiliated Hospital of Fujian Medical University

Tian Xia

Xiamen University

Shao-rong Chen

Second Affiliated Hospital of Fujian Medical University

Hongzhi Gao

Second Affiliated Hospital of Fujian Medical University

Qi-yang Shi

Second Affiliated Hospital of Fujian Medical University

shu Lin

Second Affiliated Hospital of Fujian Medical University

Research

Keywords: autologous adipose-derived stem cells, ShakeGel™3D, intrauterine adhesion, BMP7-Smad5 signaling pathway

Posted Date: January 19th, 2021

DOI: <https://doi.org/10.21203/rs.3.rs-146857/v1>

License:   This work is licensed under a Creative Commons Attribution 4.0 International License.

[Read Full License](#)

Version of Record: A version of this preprint was published on March 18th, 2021. See the published version at <https://doi.org/10.1186/s13287-021-02258-0>.

Abstract

Background: The objective was to explore the therapeutic effect of autologous adipose-derived stem cells (ADSCs) combined with ShakeGel™3D transplantation to activate the BMP7-Smad5 signaling pathway to treat intrauterine adhesions (IUA).

Methods: Autologous ADSCs were isolated and then merged with ShakeGel™3D. The IUA model was established by mechanical injury. The third generation of autologous ADSCs was injected directly into the uterus in combination with ShakeGel™3D. After 7 days of treatment, endometrial morphology, number of endometrial glands, endometrial fibrosis area, and fibrosis biomarker analysis by RT-PCR and IHC were examined. BMP7 and phosphorylation of Smad5 were also detected, and the recovery of infertility function in treated mice was evaluated.

Results: Fluorescence-activated cell sorting (FACS) showed that autologous ADSCs expressed CD105 (99.1%), CD29 (99.6%) and CD73 (98.9%). Autologous ADSCs could still maintain a good growth state in ShakeGel™3D. Histological examination revealed that the number of endometrial glands increased significantly, and the area of fibrosis decreased. At the same time, the expression of BMP7 and Smad5 in the ADSCs + Gel group was significantly upregulated, and the final reproductive function recovered to about 70%.

Conclusions: Autologous ADSCs can be used in combination with ShakeGel™3D to maintain functionality and create a viable three-dimensional growth environment. The combined transplantation of autologous ADSCs and ShakeGel™3D promotes the recovery of damaged endometrial tissue by increasing BMP7-Smad5 signal transduction, resulting in endometrium thickening, increased number of glands, and decreased fibrosis, leading to restoration of partial fertility.

1. Background

Intrauterine adhesions (IUA), the most common cause of uterine infertility, partially or completely block the uterine cavity and/or cervical canal and are caused by endometrial basal layer injury. There are several hypotheses about the pathogenesis of IUA, including the fibrosis hyperplasia theory, the neural reflex theory, abnormal differentiation of stem cells, changes in the uterine microenvironment and fibrosis, abnormal regulation of signaling pathways, and inflammatory response caused by adherent fibroblasts. Since the pathological features of IUA are endometrial fibrosis, the fibrosis hyperplasia theory is the most widely studied hypothesis. As a serious complication of uterine surgery, IUA can cause a plethora of female reproductive system health problems, such as menstrual abnormalities, recurrent abortion, periodic abdominal pain, infertility and pregnancy-related complications. Therefore, the goal of IUA therapy is to reconstruct the normal uterine cavity and restore uterine function. The traditional treatment for this disease is hysteroscopic resection of transcervical adhesion, combined with various adjuvant therapies. However, some shortcomings and deficiencies of these anti-adhesion strategies, such as resistance to secondary surgery, limited isolation area, induction of intrauterine inflammatory response,

and difficulty in endometrial regeneration, have forced researchers to continue to explore new treatment options.

Mesenchymal stem cells (MSCs) have the ability of multipotent differentiation, they can promote tissue repair, and are characterized by low immunoreactivity and high immunosuppression. They are a suitable source of stem cells for the treatment of intrauterine adhesions. However, the safety of allogeneic MSCs regeneration therapy remains controversial. Compared with autologous MSCs, allogeneic MSCs have a higher risk of initiating an immune response [1], higher morbidity [2], and secondary cancers that may occur after allogeneic stem cell transplantation [3]. According to recent experiments and reports, autologous MSCs seem to be more suitable for the treatment of diseases [4–7]. Adipose-derived stem cells (ADSCs), a type of MSCs, have shown promise in regenerative medicine. In preclinical animal models, autologous ADSCs are used to repair articular cartilage defects [8], enhance the recovery of erectile function after cavernous nerve injury [9] and repair Achilles tendon defects [10]. Furthermore, autologous ADSCs have been used in the treatment of Crohn's disease anal fistula [11], systemic sclerosis [12], and tracheo-oesophageal fistula in humans [13]. In addition, we reviewed the application of MSCs in female reproductive diseases [14]. Currently, the primary mechanisms of MSCs therapy have not been fully elucidated. The main mechanisms include differentiation into targeted cells, immunomodulatory interactions with multiple immune cells, homing and engraftment at targeted injury sites, and paracrine effects of various factors, among which the paracrine effect is the most likely mode of action.

In order to improve the local persistence and utilization rate of MSCs in the endometrium, scientists have used materials such as collagen scaffolds [15–17], hydrogel scaffolds [18], and platelet-rich plasma [19] to loaded with MSCs to restore the structure and function of the endometrium. Our experiments used a material with a three-dimensional polymeric network, a bioactive hydrogel mimicking the microenvironment and microstructure of tissues, supporting 3D tissue-like growth *in vitro* and *in vivo* [20]. ShakeGelTM3D can also improve the proliferation or differentiation of stem cells.

Bone morphogenetic protein 7 (BMP7) is a member of the transforming growth factor (TGF) superfamily and a natural negative regulator of the TGF- β /Smad signaling pathway. Recently, a number of studies have found that BMP7 can inhibit the progression of cardiac fibrosis [21], glomerular and interstitial fibrosis in mouse models of chronic renal disease [22, 23], pulmonary fibrosis [24], and IUA [25]. Furthermore, experiments have shown that BMP7 may suppress TGF- β 1, which mediates IUA fibrosis by stimulating Smad and downstream regulatory pathways [26–30], inducing the process by regulating Smad5 to repair tissues [25].

In this study, we evaluated the therapeutic effects of a complex of mouse autologous ADSCs loaded on ShakeGelTM3D in an IUA mouse model by activating the BMP7-Smad5 signaling pathway, which increased local perseverance and stem cells activity. We also aimed to analyze whether transplantation of autologous ADSCs combined with ShakeGelTM3D could improve the fertility of IUA mice.

2. Materials And Methods

2.1 Experimental animals

All animal experimental protocols were approved by the Second Affiliated Hospital of Fujian Medical University Animal Care Committee and were in accordance with the National Institutes of Health Guide for the Care and Use of Laboratory Animals (number 97). Mice were kept in standard cages at 22 °C with a 12 h light-dark cycle and were allowed unlimited access to food and water.

2.2 Autologous ADSCs preparation and identification

Mouse autologous ADSCs were prepared and cultured as described in previous studies [31–33]. Briefly, inguinal adipose tissue was obtained from female C57BL/6 mice 3–4 weeks of age, and each mouse was given an ear tag with a certain number on it. Fat tissue was collected and enzymatically digested with 0.75 mg/mL collagenase type I (Sigam) for 30 min at 37 °C. Immediately after digestion, the sample was centrifuged, and the precipitate was retained. For culture, the precipitate was rinsed twice in PBS, and the cell pellet was re-suspended in DMEM/F12 (1:1) (Hyclone) containing 10% fetal bovine serum (Gibco), 1% pen-strep (Gibco) and cultured at 37 °C in a 5% CO₂ humidified incubator. Flow cytometric analysis was used to identify cell surface markers of ADSCs, including CD105 (BioLegend), CD29 (BioLegend), CD75 (BioLegend), CD34 (BioLegend) and CD45 (BioLegend). Cells were treated with commercial osteogenic, chondrogenic, or adipogenic medium (Cyagen) for up to 24 days, following the manufacturer's instructions. The ability of ADSCs to differentiate through adipogenesis, osteogenesis and chondrogenesis was visualized by Oil Red O staining, Alizarin red staining and Alcian blue staining (Cyagen), respectively. Autologous ADSCs from passage 3 were used for experiments.

2.3 Preparation of the mouse autologous ADSCs combined with ShakeGel™3Dcomplex

The complex was made as follows: First, the ShakeGel™3D (Biomaterials USA) solution, which has been reported to improve cell culture strategies [20], was gently mixed with the cell suspension into a centrifuge tube. Second, cell culture wells were pre-wet with 1× sterile PBS, and then the gel-cell mixture was rapidly added to the well and the mix was gently rocked back and forth to spread the mixture evenly across the surface of the well. Third, incubation followed at 37 °C for 5-10 min for hydrogel formation. Fourth, culture medium was added along the plate wall, followed by incubation at 37 °C in a humidified atmosphere containing 5% CO₂. Finally, after 24 h, half the volume of the old medium was discarded, and the same amount of fresh medium was added. After that, the medium was refreshed every 24 h. According to the manufacturer's protocol, Calcein AM (Abcam) was used to examine cell viability, and cell counting Kit-8 (CCK-8) (Dojindo) was used to evaluate the proliferation of ADSCs. Three samples from each group were assessed using the CCK-8 assay (n = 3).

2.4 Establishment of IUA model

When the cells reached the second generation, which is about six or seven weeks in mice, the IUA mouse model was established according to previous research [34]. Seven days after the surgery, the autologous ADSCs were cultured to the third generation. The mice (n = 50) were subdivided into 5 groups: sham operation group (sham group, n = 10), where mice had laparotomy without any treatment; PBS model group (PBS group, n = 10), where mice underwent induction of intrauterine adhesions, and, seven days after modeling, a relaparotomy was performed and the mice were injected with 10 μ l PBS in each of the two uterine horns; autologous ADSCs treatment group (ADSCs group, n = 10), where a relaparotomy was performed after seven days of modeling, and autologous ADSCs (5×10^6 suspended in 10 μ l PBS) [35] were injected into each of the two uterine horns, one by one, according to the mouse's ear tag; ShakeGelTM3D model group (Gel group, n = 10), where mice underwent induction of intrauterine adhesions seven days after modeling, a relaparotomy was performed, and the mice were injected with 10 μ l ShakeGelTM3D in each of the two uterine horns; and ADSCs combined with ShakeGelTM3D treatment group (ADSCs + Gel group, n = 10), where a relaparotomy was performed after 7 days of modeling, and ADSCs combined with ShakeGelTM3D (5×10^6 suspended in 10 μ l ShakeGelTM3D) were injected into each of the two uterine horns, one by one, according to the mouse's ear tag. Seven days after treatment, 25 mice (n = 5 per group) were sacrificed, their uterine tissues were harvested for the next experiment, and the other 25 remained for mating experiments. The study design is shown in Fig. 1.

2.5 GFP labeling of ADSCs

The green fluorescent protein (GFP) of a lentivirus (OBIO Technology) was stored at - 80 °C. According to the manufacturer's protocol, after 72 h of virus infection, the cells were observed under a fluorescence microscope to determine the efficiency of cell infection. These cells were then injected into the uterus.

2.6 Hematoxylin & eosin (H&E) staining

Uteri were fixed in 4% paraformaldehyde for 24 h and embedded in paraffin. The slides were first deparaffinized and rehydrated, and then stained with H&E (Solarbio). We visualized the whole image of the pathological uterus and counted the gland quantity to predict IUA.

2.7 Masson staining

Masson staining was used to detect endometrial fibrosis. The deparaffinized and rehydrated slides were incubated with Masson staining mixture (Solarbio) for 5 min and then stained with phosphomolybdic acid-aniline blue solution (Solarbio) for 5 min. The areas of the collagen fibers stained in blue relative to the total view were calculated.

2.8 Quantitative real-time polymerase chain reaction (qRT-PCR)

Total RNA was extracted from macrophages using the Mini BEST Universal RNA Extraction Kit (TaKaRa). RNA purity and concentration were measured using a spectrophotometer. Reverse transcription and cDNA

synthesis were performed using PrimeScript™ RT reagent Kit with gDNA Eraser (Perfect Real Time) (Takara, Japan) according to the manufacturer's instructions. The mRNA expression of α -SMA, TGF- β 1, Smad-5, BMP7 was quantified by qRT-PCR with TB Green® Premix Ex Taq™ (TliRNaseH Plus) (Takara), and the housekeeping gene, glyceraldehyde 3-phosphate dehydrogenase (GAPDH), was used as an internal control for mRNA abundance. The sequences of the forward and reverse primers are shown in Table 1. Each group included six samples, and each sample was performed in triplicate. Relative gene expression between groups was calculated using the $2^{-\Delta\Delta CT}$ method.

Table 1
qRT-PCR Forward/Reverse(F/R) primers sequences.

Primers	Sequences 5'-3'
a-SMA	F: 5'- GCGTGGCTATTCCTTCGTGACTAC - 3'
	R: 5'- CGTCAGGCAGTTCGTAGCTCTTC - 3'
TGF- β 1	F: 5'- CCAGATCCTGTCCAAACTAAGG - 3'
	R: 5'- CTCTTTAGCATAGTAGTCCGCT - 3'
BMP7	F: 5'- GATCCTGTCCATCTTAGGGTTG - 3'
	R: 5'- GTTGTACAGGTCCAACATGAAC - 3'
Smad5	F: 5'- TTTCCCCTTATCTCCTAACAGC - 3'
	R: 5'- TACTGCTTGTATCCATAGGCTG - 3'
GAPDH	F: 5'- TGGGTGTGAACCATGAGAAG-3'
	R: 5'- GCTAAGCAGTTGGTGGTGC-3'
a-SMA, α-smooth muscle actin; TGF-β1, transforming growth factor beta receptor I BMP7, bone morphogenetic protein 7; Smad5, SMAD family member 5; GAPDH, glyceraldehyde-3-phosphate dehydrogenase.	

2.9 Immunohistochemistry

After deparaffinization, dehydration and antigen retrieval, the slides were immersed in 3% hydrogen peroxide to block endogenous peroxidase activity, and then they were blocked in goat serum for 1 h. The slides were then incubated overnight at 4 °C with primary antibodies against α -smooth muscle actin (α -SMA, Abcam, 1:2000), TGF- β 1 (Abcam, 1:500), BMP7 (Abcam, 1 μ g/ml), and Smad5 (Abcam, 1:800). The sections were then incubated with appropriate secondary antibodies for 60 min at room temperature. The slides were then stained with 3, 3-diaminobenzidine (DAB) at room temperature, lightly counterstained with hematoxylin, dehydrated and covered with glass cover slips. Quantification of immunoreactivity was performed using Image Pro-Plus 6.0, and 3–5 fields were randomly selected from each slide to determine the mean optical density (MOD).

2.10 Statistical analysis

Data were analyzed using the F test with subsequent t-tests (equal variance) for the comparison between two different groups. For three or more groups, an ANOVA test was used, followed by the least significant differences method. GraphPadPrism8 (GraphPad Software Inc., La Jolla, CA, USA) was used to obtain graphs and statistics. Significant values were designated as follows: * $p < 0.05$, ** $p < 0.01$, *** $P < 0.001$, and **** $P < 0.0001$. All data are shown as the mean \pm standard deviation (SD).

3. Results

3.1 Characterization and differentiation of autologous ADSCs and their safety assessment on ShakeGel™3D

The appearance of autologous ADSCs from passage 0 (P0) to P3, especially the third passage, gradually came to resemble typical spindle-shaped fibroblast-like cells that were arranged closely with vortex-like growth (Fig. 2.1). In the third passage, fluorescence-activated cell sorting (FACS) showed that autologous ADSCs expressed CD105 (99.1%), CD29 (99.6%), and CD73 (98.9%), and few were positive for CD34 and CD45 (Fig. 2.2). In addition, these cells were successfully induced to become adipocytes, osteoblasts and chondroblasts *in vitro* (Fig. 2.3).

To further evaluate the safety of autologous ADSCs on ShakeGel™3D, the live-dead cell staining results (Fig. 3.1) showed that these cells showed aggregation of globulin in the ShakeGel™3D, and a small number of fibrous fat stem cells were extended at the junction between the ShakeGel™3D edge and the cell culture base. On day seven in the ShakeGel™3D culture environment, autologous ADSCs showed good activity and could continue to proliferation in the shaker environment. In addition, the CCK-8 results (Fig. 3.2) verified that the OD value of cells cultured by 5×10^6 cells + ShakeGel™3D was higher than that by 1×10^6 cells + ShakeGel™3D. On the third day of co-culture, the OD value began to increase gradually. By the seventh day, the OD value of 5×10^6 cells + ShakeGel™3D was over 50%.

3.2 The IUA models the effect of autologous ADSCs on ShakeGel™3D

First, to locate the autologous ADSCs/ GFP in the uterus, as expected, we did not observe any GFP-positive cells in the uterine tissue sections of the sham, PBS, and Gel groups. However, we observed GFP-positive cells in the uterine tissue sections of the ADSCs group (2.175%) and ADSCs + Gel group (9.215%). Furthermore, GFP-positive cells in the uterine tissue sections of the ADSCs + Gel group were higher than that in the ADSCs group ($P = 0.0101$) (Fig. 4).

The macroscopic appearance of the uterus sham groups was smoother than in the PBS group. On day 7 from ADSCs transplantations, ShakeGel™3D, or ADSCs combined with ShakeGel™3D, the macroscopic

appearance of the uterus gradually recovered, similar to that of a normal uterus (Fig. 5.1). H&E staining of the uterine tissue showed that the endometrial thickness ($163.8 \pm 6.128 \mu\text{m}$) of the PBS group showed significant differences when compared with the thickness ($264.5 \pm 31.75 \mu\text{m}$) of the sham group ($P < 0.0001$, $n = 7$; Fig. 5.2). When transplanted with ADSCs or ADSCs combined with ShakeGel™3D, thickness increased significantly compared to the PBS group (ADSCs group $190.1 \pm 8.389 \mu\text{m}$, $P \leq 0.05$; ADSCs + Gel group $228.8 \pm 2.254 \mu\text{m}$, $P \leq 0.0001$). The endometrium regenerated in the ADSCs + Gel group was thicker than that in the ADSCs group ($p < 0.001$, $n = 7$) (Fig. 5.2). Further, when comparing to endometrial tissues of the PBS group, gland numbers were increased in the ADSCs group (9.182 ± 2.857 versus 1.545 ± 0.9342 , respectively, per unit area, $P < 0.0001$), Gel group (14.55 ± 1.293 versus 1.545 ± 0.9342 , respectively, per unit area, $P < 0.0001$), and ADSCs + Gel group (19.36 ± 2.063 versus 1.545 ± 0.9342 , respectively, per unit area, $P < 0.0001$). Compared with the ADSCs group, the gland numbers of ADSCs + Gel were increased ($P < 0.0001$). To further evaluate the degree of fibrosis, Masson's trichrome staining was performed. As shown in Fig. 5.3, a large amount of fibrous tissue appeared in the PBS group ($56.89 \pm 0.4425\%$), compared to the sham group ($29.44 \pm 5.2305\%$). Interestingly, the percentage of fibrosis area was decreased after ADSCs ($50.10 \pm 1.280\%$, $P < 0.05$), ShakeGel™3D ($45.17 \pm 1.196\%$, $P < 0.0001$) or ADSCs combined with ShakeGel™3D ($39.55 \pm 0.4125\%$, $P < 0.0001$) treatment compared with the PBS group. In addition, the percentage of fibrosis area in the ADSCs + Gel group was significantly less than that of the ADSCs group ($P < 0.001$).

To further confirm the results of the fibrosis of experiments, we detected α -SMA expression and α -SMA immunoreactivity (Fig. 6). All these valuations indicated that the fibrosis in the ADSCs + Gel group was significantly smaller than in the ADSCs group. In addition, expression of TGF- β 1, an archetypical promoter of fibrosis, (Fig. 6.2-b) was significantly less in the ADSCs + Gel group than in the ADSCs group, as shown by qRT-PCR (Fig. 7.1-b) and IHC experiments. The mating experiments showed that only the Sham group and ADSCs + Gel group achieved pregnancy (Fig. 7.2).

3.3 ADSCs combined with ShakeGel™3D treatment enhance BMP7-Smad5 signaling

The qRT-PCR results (Fig. 7.1) showed that BMP7 expression in the ADSCs group (0.06124 ± 0.006388) was slightly higher than in the PBS group (0.05062 ± 0.01281), but the difference was not statistically significant ($P = 0.5302$). BMP7 expression was higher in ADSCs + Gel group (0.5575 ± 0.06289) than in the PBS group. The difference was statistically significant ($P < 0.0001$). The ADSCs + Gel group was also statistically significant compared to the ADSCs group ($P < 0.0001$). Similarly, Smad5 expression in the ADSCs group (0.7127 ± 0.05734) was slightly higher than in the PBS group (0.6843 ± 0.07691), but the difference was not statistically significant ($P = 0.9820$). The mRNA expression of Smad5 in the ADSCs + Gel group (0.9066 ± 0.07593) was significantly higher than in the PBS group ($P < 0.01$). The ADSCs + Gel group result was also statistically significant compared with ADSCs ($P = 0.0167$).

Likewise, for immunohistochemistry results, the staining intensity for BMP7 in the ADSCs group (0.02330 ± 0.006284) was slightly higher than that in the PBS group (0.002817 ± 0.002115), but the difference was

not statistically significant ($P = 0.1739$). BMP7 expression was higher in the ADSCs + Gel group (0.1314 ± 0.01210) than in the PBS group. The difference was statistically significant ($P < 0.0001$). Compared with the ADSCs group, the ADSCs + Gel group expression was significantly higher ($P < 0.0001$). The mean density of Smad5 in the PBS group (0.1676 ± 0.06002) was lower than in the ADSCs group (0.2391 ± 0.02442 , $P < 0.0001$), Gel group (0.2910 ± 0.009053 , $P < 0.0001$), and ADSCs + Gel group (0.3372 ± 0.004266 , $P < 0.0001$). The mean density of Smad5 in the ADSCs group was significantly higher than in the ADSCs group ($P < 0.0001$) and Gel group ($P = 0.0087$).

4. Discussion

In this study, three main points were observed. First, the combination of ShakeGelTM3D and autologous ADSCs can achieve good results, thereby creating a feasible three-dimensional growth environment. Second, autologous ADSCs combined with ShakeGelTM3D can promote the recovery of injured endometrial tissue, thus increasing the thickness of the endometrium, increasing the number of glands and reducing fibrosis. Third, compared with other treatment groups, the combination of autologous ADSCs and ShakeGelTM3D grafts can increase the expression of BMP7 and Smad5, indicating that the combination of autologous ADSCs and ShakeGelTM3D grafts can promote endometrial repair through the BMP7-Smad5 signaling pathway.

Stem cells, including MSCs, are one of the most promising tools, and they have been applied to various tissues for regenerative medicine and cell therapy, such as the uterus [36, 37]. ADSCs can be isolated from adipose tissue in large quantities, and autologous transplantation can be realized. Some studies have shown that the application of allogeneic stem cell therapy has some risks, including abnormal immune reconstitution, secondary cancer and graft-versus-host disease [3, 38, 39]. Our study is the first to use autologous ADSCs to treat intrauterine adhesions in mice. In our study, we used autologous ADSCs combined with ShakeGelTM3D, which has proven that it can support the microenvironment and tissue microstructure for cells to improve proliferation [20]. The CCK-8 results of our study showed that autologous ADSCs still proliferate in ShakeGelTM3D. Furthermore, the effects of the group with autologous ADSCs combined with ShakeGelTM3D were confirmed by histological inspection and detection of some fiber correlation factors. In addition, compared with the ADSCs and the Gel groups, the ADSCs + Gel group had more GFP-positive cells in the endometrial tissue, thickened endometrium, increased endometrial glands, decreased fibrotic area, and α -SMA and TGF- β 1 expression. These results suggest that the ShakeGelTM3D not only acts as a physical barrier to IUA, but also provides an ideal attachment site for ADSCs to maintain a high density in the uterine cavity, thereby improving reconstruction of abnormal tissue. Although Liu et al. concluded that systemic administration can recruit MSCs to the injured uterus better than local injection [40], vein engraftment of stem cells in the damaged area cannot be guaranteed. In fact, the majority of the stem cells after intravenous injection are trapped in the lungs, and the number of MSCs that home to the endometrium is very small [41, 42]. In addition, in our research, ShakeGelTM3D serves as a slow-release stem cell scaffold, allowing ADSCs to continuously

secrete factors to promote endometrial repair. Therefore, we used local injection of autologous ADSCs combined with ShakeGel™3D to treat IUA.

Abnormal repair and fibrosis after endometrial surgery can lead to intrauterine adhesion damage, which is pathologically similar to all fibrotic lesions, including the extracellular matrix, excessive accumulation of tissue remodeling, and scar formation[43]. Therefore, for IUA therapy, blocking the formation of fibrosis plays a key role. TGF-β1 has been shown to promote endometrial fibrosis in IUA patients and animal models [44]. However, a previous study showed that the expression of BMP7, another member of the TGF-β superfamily, was reduced in IUA. BMP7-Smad5 signal transduction occurs in endometrial fibrosis and has an anti-fibrotic effect in IUA [25]. Our study used mechanical trauma to establish a mouse model of IUA. We found that, compared with the PBS group, both the mRNA and protein BMP7 levels in the ADSCs + Gel group increased. At the same time, the level of Smad5 consistent with that of BMP7 also increased. Compared with the PBS group, the levels of BMP7 and Smad5 in the ADSCs group increased slightly, but the difference was no statistically significant. Our study shows for the first time that the combination of ADSCs and ShakeGel™3D can treat IUA by changing the BMP7-Smad5 signaling pathway. Furthermore, we suggest that the gel can improve the function of ADSCs.

We outline next few steps in our ongoing research to further elucidate the mechanism of ADSCs combined with gel in the treatment of intrauterine adhesions. First, due to the extreme challenge of preparing an appropriate number of autologous ADSCs, we plan to isolate and purify exosomes from ADSCs in place of cell therapy for IUA. In addition, we may be able to identify key factors in the release of ADSCs during endometrial recovery. Second, we have just completed a mouse study, and we are planning to treat IUA with autologous ADSCs combined with ShakeGel™3D in a large animal model more similar to the pathophysiology of the endometrium of human females. In addition, randomized controlled trials are needed to confirm the therapeutic role of ADSCs in fertility medicine.

5. Conclusion

In this study, it was shown that both autologous ADSCs and autologous ADSCs combined with ShakeGel™3D could repair IUA caused by mechanical injury. Since ShakeGel™3D enhances the function of ADSCs, autologous ADSC transplantation combined with ShakeGel™3D holds significant advantages in anti-fibrotic repair and promotion of endometrial regeneration by altering the BMP7-Smad5 signaling pathway. These data are helpful in treating intrauterine adhesions.

Abbreviations

Intrauterine adhesions (IUA); Mesenchymal stem cells (MSCs); Adipose-derived stem cells (ADSCs); Bone morphogenetic protein 7 (BMP7); transforming growth factor (TGF)

Declarations

Ethics approval and consent to participate

All animal procedures reported in this study have been approved by the Second Affiliated Hospital of Fujian Medical University Animal Care Committee under protocol number 97.

Consent for publication

Not applicable

Availability of data and materials

The data that support the findings of this study are available from the corresponding author upon reasonable request.

Competing interests

There is no conflict of interest to declare.

Funding

This work was supported by BS202007, 2018N019S, and 2018-CX-34.

Authors' contributions

Shu Lin, Qi-yang Shi, Hongzhi Gao, and Shao-rong Chen designed the study methodology. Yuan-xia Zao, Qiao-yi Huang, Wei-can Chen and Tian Xia collected the data and analyzed the results. Yuan-xia Zao drafted the article. All authors reviewed and revised the work. All authors reviewed the final article and approved it for submission.

Acknowledgements

Not applicable.

References

1. Rowe JM, Ciobanu N, Ascensao J, Stadtmauer EA, Weiner RS, Schenkein DP, et al. Recommended Guidelines for the Management of Autologous and Allogeneic Bone Marrow Transplantation A Report from the Eastern Cooperative Oncology Group (ECOG). 2018;143–58.
2. Majhail NS, Mau LW, Denzen EM, Arneson TJ. Costs of autologous and allogeneic hematopoietic cell transplantation in the United States: a study using a large National Private Claims Database. 2013;294–300.
3. B M, M M. Long-term complications and side effects after allogeneic hematopoietic stem cell transplantation: an update. Blood Cancer J [Internet]. Blood Cancer J; 2011 [cited 2020 Nov 30];1. Available from: <http://www.ncbi.nlm.nih.gov/pubmed/22829137>

4. Lu M, Peng L, Ming X, Wang X, Cui A, Li Y, et al. Enhanced wound healing promotion by immune response-free monkey autologous iPSCs and exosomes vs. their allogeneic counterparts. *EBioMedicine* [Internet]. Elsevier B.V.; 2019;42:443–57. Available from: <https://doi.org/10.1016/j.ebiom.2019.03.011>
5. Riccobono D, Agay D, Scherthan H, Forcheron F, Vivier M, Ballester B, et al. Application of adipocyte-derived stem cells in treatment of cutaneous radiation syndrome. *Health Phys.* 2012;103:120–6.
6. Osborn TM, Hallett PJ, Schumacher JM, Isacson O. Advantages and Recent Developments of Autologous Cell Therapy for Parkinson's Disease Patients. *Front Cell Neurosci.* 2020;14:1–13.
7. Chang YW, Wu YC, Huang SH, Wang HMD, Kuo YR, Lee SS. Autologous and not allogeneic adipose-derived stem cells improve acute burn wound healing. *PLoS One.* 2018;13:1–16.
8. Li Q, Zhao F, Li Z, Duan X, Cheng J, Zhang J, et al. Autologous Fractionated Adipose Tissue as a Natural Biomaterial and Novel One-Step Stem Cell Therapy for Repairing Articular Cartilage Defects. *Front Cell Dev Biol.* 2020;8:1–15.
9. X Q, TM F, L F, M A, H O, H Z, et al. Both immediate and delayed intracavernous injection of autologous adipose-derived stromal vascular fraction enhances recovery of erectile function in a rat model of cavernous nerve injury. *Eur Urol* [Internet]. *Eur Urol*; 2012 [cited 2020 Nov 30];62. Available from: <http://www.ncbi.nlm.nih.gov/pubmed/22397847>
10. Deng D, Wang W, Wang B, Zhang P, Zhou G, Zhang WJ, et al. Repair of Achilles tendon defect with autologous ASCs engineered tendon in a rabbit model. *Biomaterials* [Internet]. *Biomaterials*; 2014 [cited 2020 Nov 30];35:8801–9. Available from: <http://www.ncbi.nlm.nih.gov/pubmed/25069604>
11. Dige A, Hougaard HT, Agnholt J, Pedersen BG, Tencerova M, Kassem M, et al. Efficacy of Injection of Freshly Collected Autologous Adipose Tissue Into Perianal Fistulas in Patients With Crohn's Disease. *Gastroenterology* [Internet]. *Gastroenterology*; 2019 [cited 2020 Nov 30];156:2208-2216.e1. Available from: <http://www.ncbi.nlm.nih.gov/pubmed/30772343>
12. Granel B, Daumas A, Jouve E, Harlé J-R, Nguyen P-S, Chabannon C, et al. Safety, tolerability and potential efficacy of injection of autologous adipose-derived stromal vascular fraction in the fingers of patients with systemic sclerosis: an open-label phase I trial. *Ann Rheum Dis* [Internet]. *Ann Rheum Dis*; 2015 [cited 2020 Nov 30];74:2175–82. Available from: <http://www.ncbi.nlm.nih.gov/pubmed/25114060>
13. PD A, M G-A, T G-H, D G-O. A new bronchoscopic treatment of tracheomediastinal fistula using autologous adipose-derived stem cells. *Thorax* [Internet]. *Thorax*; 2008 [cited 2020 Nov 30];63. Available from: <http://www.ncbi.nlm.nih.gov/pubmed/18364447>
14. Zhao Y-X, Chen S-R, Su P-P, Huang F-H, Shi Y-C, Shi Q-Y, et al. Using Mesenchymal Stem Cells to Treat Female Infertility: An Update on Female Reproductive Diseases. *Stem Cells Int* [Internet]. *Stem Cells Int*; 2019 [cited 2020 Dec 3];2019:9071720. Available from: <http://www.ncbi.nlm.nih.gov/pubmed/31885630>
15. Zhao G, Cao Y, Zhu X, Tang X, Ding L, Sun H, et al. Transplantation of collagen scaffold with autologous bone marrow mononuclear cells promotes functional endometrium reconstruction via

- downregulating Δ Np63 expression in Asherman's syndrome. *Sci China Life Sci.* 2017;60:404–16.
16. Xin L, Lin X, Pan Y, Zheng X, Shi L, Zhang Y, et al. A collagen scaffold loaded with human umbilical cord-derived mesenchymal stem cells facilitates endometrial regeneration and restores fertility. *Acta Biomater* [Internet]. *Acta Materialia Inc.*; 2019;92:160–71. Available from: <https://doi.org/10.1016/j.actbio.2019.05.012>
 17. Cao Y, Sun H, Zhu H, Zhu X, Tang X, Yan G, et al. Allogeneic cell therapy using umbilical cord MSCs on collagen scaffolds for patients with recurrent uterine adhesion: A phase i clinical trial. *Stem Cell Res Ther.* 2018;9:1–10.
 18. Huang Q, Zou Y, Arno MC, Chen S, Wang T, Gao J, et al. Hydrogel scaffolds for differentiation of adipose-derived stem cells. *Chem Soc Rev* [Internet]. Royal Society of Chemistry; 2017;46:6255–75. Available from: <http://dx.doi.org/10.1039/C6CS00052E>
 19. Zhang S, Li P, Yuan Z, Tan J. Platelet-rich plasma improves therapeutic effects of menstrual blood-derived stromal cells in rat model of intrauterine adhesion. *Stem Cell Res Ther.* 2019;10:1–12.
 20. Chen H, Wei X, Chen H, Wei H, Wang Y, Nan W, et al. The study of establishment of an in vivo tumor model by three-dimensional cells culture systems methods and evaluation of antitumor effect of biotin-conjugated pullulan acetate nanoparticles. *Artif Cells, Nanomedicine Biotechnol* [Internet]. Taylor & Francis; 2019;47:123–31. Available from: <https://doi.org/10.1080/21691401.2018.1544142>
 21. Towbin JA. Scarring in the Heart – A Reversible Phenomenon? *N Engl J Med.* 2007;357:1767–8.
 22. Zeisberg M, Hanai JI, Sugimoto H, Mammoto T, Charytan D, Strutz F, et al. BMP-7 counteracts TGF- β 1-induced epithelial-to-mesenchymal transition and reverses chronic renal injury. *Nat Med.* 2003;9:964–8.
 23. Lin J, Patel SR, Cheng X, Cho EA, Levitan I, Ullenbruch M, et al. Kielin/chordin-like protein, a novel enhancer of BMP signaling, attenuates renal fibrotic disease. *Nat Med.* 2005;11:387–93.
 24. Myllärniemi M, Lindholm P, Ryyänänen MJ, Kliment CR, Salmenkivi K, Keski-Oja J, et al. Gremlin-mediated Decrease in Bone Morphogenetic Protein Signaling Promotes Pulmonary Fibrosis. *Am J Respir Crit Care Med.* 2008;177:321–9.
 25. Guo LP, Chen LM, Chen F, Jiang NH, Sui L. Smad signaling coincides with epithelial-mesenchymal transition in a rat model of intrauterine adhesion. *Am J Transl Res.* 2019;11:4726–37.
 26. Yao Y, Chen R, Wang G, Zhang Y, Liu F. Exosomes derived from mesenchymal stem cells reverse EMT via TGF- β 1/Smad pathway and promote repair of damaged endometrium. *Stem Cell Res Ther. Stem Cell Research & Therapy*; 2019;10:1–17.
 27. Salma U, Xue M, Ali Sheikh MS, Guan X, Xu B, Zhang A, et al. Role of Transforming Growth Factor- β 1 and Smads Signaling Pathway in Intrauterine Adhesion. *Mediators Inflamm.* 2016;2016.
 28. Zhang Z, Li S, Deng J, Yang S, Xiang Z, Guo H, et al. Aspirin inhibits endometrial fibrosis by suppressing the TGF- β 1–Smad2/Smad3 pathway in intrauterine adhesions. *Int J Mol Med.* 2020;45:1351–60.
 29. Liu S, Huang X, Liu Y, Song D, Xiao Y. Functional analysis of miRNAs combined with TGF- β 1/Smad3 inhibitor in an intrauterine rat adhesion cell model. *Mol Cell Biochem* [Internet]. Springer US;

- 2020;470:15–28. Available from: <https://doi.org/10.1007/s11010-020-03741-7>
30. Liu L, Chen G, Chen T, Shi W, Hu H, Song K, et al. si-SNHG5-FOXF2 inhibits TGF- β 1-induced fibrosis in human primary endometrial stromal cells by the Wnt/ β -catenin signalling pathway. *Stem Cell Res Ther*. *Stem Cell Research & Therapy*; 2020;11:1–17.
 31. PA Z, M Z, H M, J H, JW F, AJ K, et al. Multilineage cells from human adipose tissue: implications for cell-based therapies. *Tissue Eng* [Internet]. *Tissue Eng*; 2001 [cited 2020 Dec 5];7. Available from: <http://www.ncbi.nlm.nih.gov/pubmed/11304456>
 32. Bunnell BA, Flaas M, Gagliardi C, Patel B, Ripoll C. Adipose-derived stem cells: Isolation, expansion and differentiation. *Methods*. 2008;45:115–20.
 33. Si Z, Wang X, Sun C, Kang Y, Xu J, Wang X, et al. Adipose-derived stem cells: Sources, potency, and implications for regenerative therapies. *Biomed Pharmacother* [Internet]. Elsevier; 2019;114:108765. Available from: <https://doi.org/10.1016/j.biopha.2019.108765>
 34. B L, Q Z, J S, D L. Human amniotic epithelial cells improve fertility in an intrauterine adhesion mouse model. *Stem Cell Res Ther* [Internet]. *Stem Cell Res Ther*; 2019 [cited 2020 Dec 5];10. Available from: <http://www.ncbi.nlm.nih.gov/pubmed/31412924>
 35. Y L, R T, N P, R M, HS T. Systemic administration of bone marrow-derived cells leads to better uterine engraftment than use of uterine-derived cells or local injection. *J Cell Mol Med* [Internet]. *J Cell Mol Med*; 2018 [cited 2020 Dec 7];22. Available from: <http://www.ncbi.nlm.nih.gov/pubmed/28782281>
 36. R A, L A-M, M N, F M, S N, M Y. Stem cell therapy in Asherman syndrome and thin endometrium: Stem cell-based therapy. *Biomed Pharmacother* [Internet]. *Biomed Pharmacother*; 2018 [cited 2020 Dec 26];102. Available from: <http://www.ncbi.nlm.nih.gov/pubmed/29571018>
 37. H C, I C, C S. Bioengineering the Uterus: An Overview of Recent Advances and Future Perspectives in Reproductive Medicine. *Ann Biomed Eng* [Internet]. *Ann Biomed Eng*; 2017 [cited 2020 Dec 26];45. Available from: <http://www.ncbi.nlm.nih.gov/pubmed/28028711>
 38. Bellm LA, Epstein JB, Rose-Ped A, Martin P, Fuchs HJ. Patient reports of complications of bone marrow transplantation. *Support Care Cancer*. 2000;8:33–9.
 39. Lamarthée B, Malard F, Saas P, Mohty M, Gaugler B. Interleukin-22 in graft-versus-host disease after allogeneic stem cell transplantation. *Front Immunol*. 2016;7:1–9.
 40. Liu Y, Tal R, Pluchino N, Mamillapalli R, Taylor HS. Systemic administration of bone marrow-derived cells leads to better uterine engraftment than use of uterine-derived cells or local injection. *J Cell Mol Med*. 2018;22:67–76.
 41. IM B, P C, J B, MS F, S E, A T, et al. Systemic delivery of bone marrow-derived mesenchymal stem cells to the infarcted myocardium: feasibility, cell migration, and body distribution. *Circulation* [Internet]. *Circulation*; 2003 [cited 2020 Dec 27];108. Available from: <http://www.ncbi.nlm.nih.gov/pubmed/12900340>
 42. J Z, Q Z, Y W, Y L. Uterine infusion with bone marrow mesenchymal stem cells improves endometrium thickness in a rat model of thin endometrium. *Reprod Sci* [Internet]. *Reprod Sci*; 2015 [cited 2020 Dec 27];22. Available from: <http://www.ncbi.nlm.nih.gov/pubmed/24947483>

43. Wynn TA, Ramalingam TR. Mechanisms of fibrosis: Therapeutic translation for fibrotic disease. Nat Med [Internet]. Nature Publishing Group; 2012;18:1028–40. Available from: <http://dx.doi.org/10.1038/nm.2807>

44. U S, M X, MS AS, X G, B X, A Z, et al. Role of Transforming Growth Factor- β 1 and Smads Signaling Pathway in Intrauterine Adhesion. Mediators Inflamm [Internet]. Mediators Inflamm; 2016 [cited 2020 Dec 26];2016. Available from: <http://www.ncbi.nlm.nih.gov/pubmed/26997760>

Figures

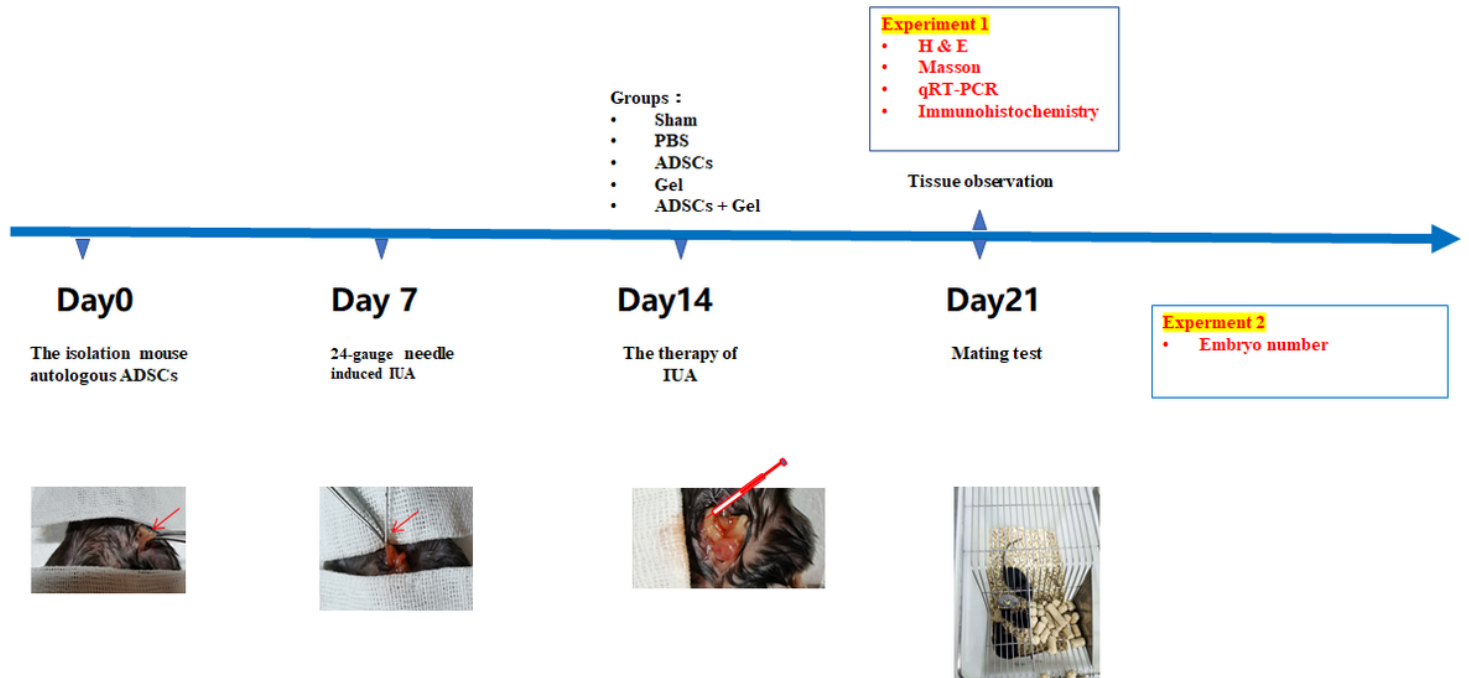


Figure 1

Study design

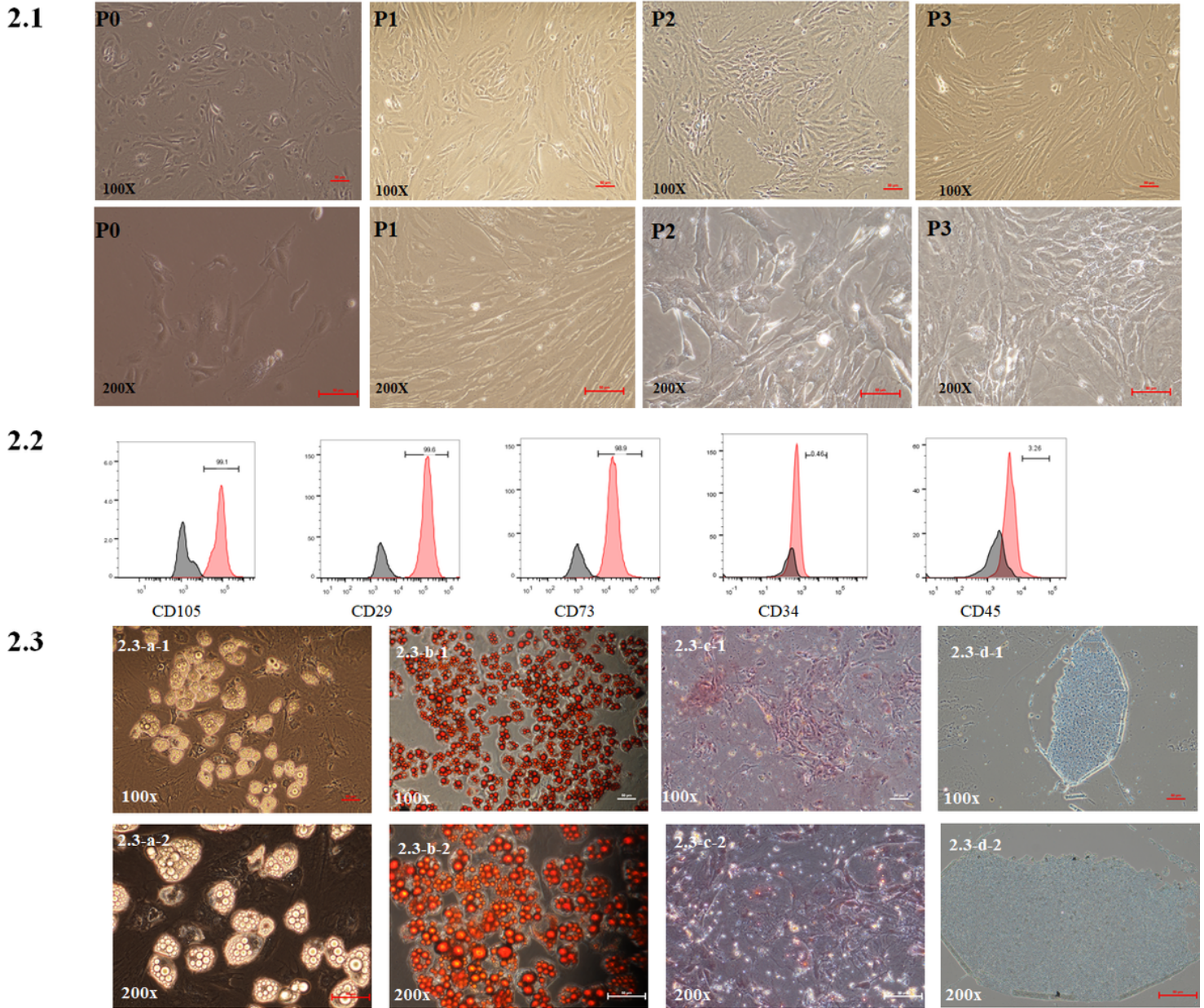


Figure 2

2.1 The appearance of autologous ADSCs of passage 0 (P0) to P3. The cells at third passage showed homogenous fibroblastic morphology. 2.2 Adipose tissue derived mesenchymal stem cell identification with flow cytometry. CD105: 99.1%, CD29: 99.6% CD73: 98.9%, CD34: 0.46%, CD45: 3.26%. 2.3 The differentiation of ADSCs. Under the white light, The differentiated adipocytes secreted lipid droplets (2.3-a-1, 2.3-a-2). Oil Red-O staining adipogenic differentiation (2.3-b-1, 2.3-b-2). Alizarin red staining indicated osteogenic differentiation (2.3-c-1, 2.3-c-2). Alcian blue staining indicated chondrogenic differentiation (2.3-d-1, 2.3-d-2).

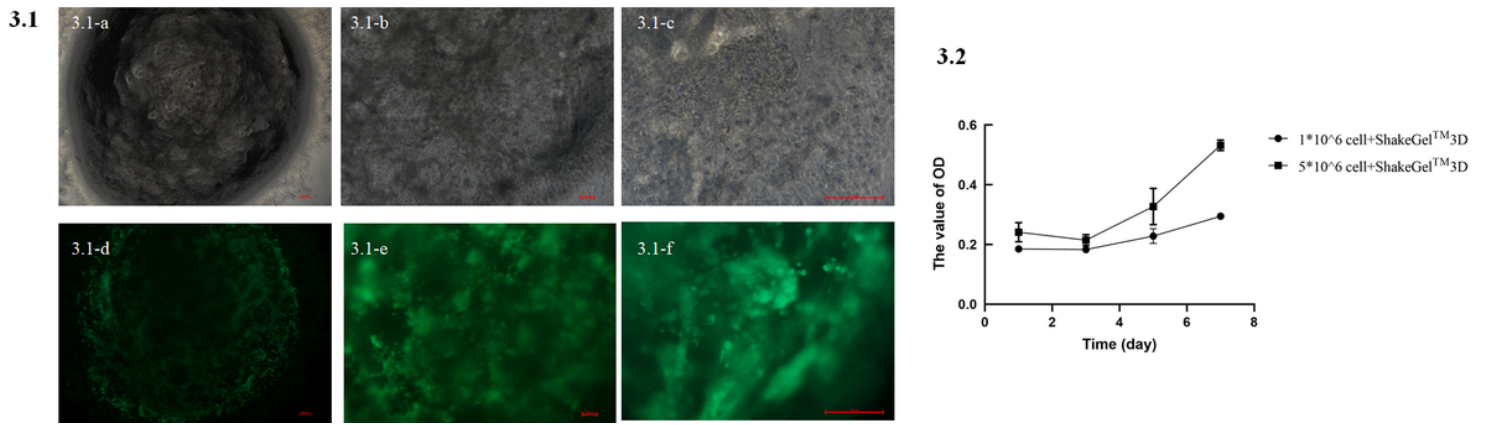


Figure 3

3.1 Assay of the activity of ADSCs combined with ShakeGelTM3D. 3.1-a, 3.1-b, and 3.1-c respectively were ADSCs combined with ShakeGelTM3D under white light 4x, 10x, 20x. 3.1-d, 3.1-e, and 3.1-f respectively were ADSCs combined with ShakeGelTM3D under active staining 4x, 10x, 20x (Scale bar=100μm). 3.2 The results of CCK-8 in 1*10⁶ ADSCs and 5*10⁶ ADSCs co-culture with ShakeGelTM3D

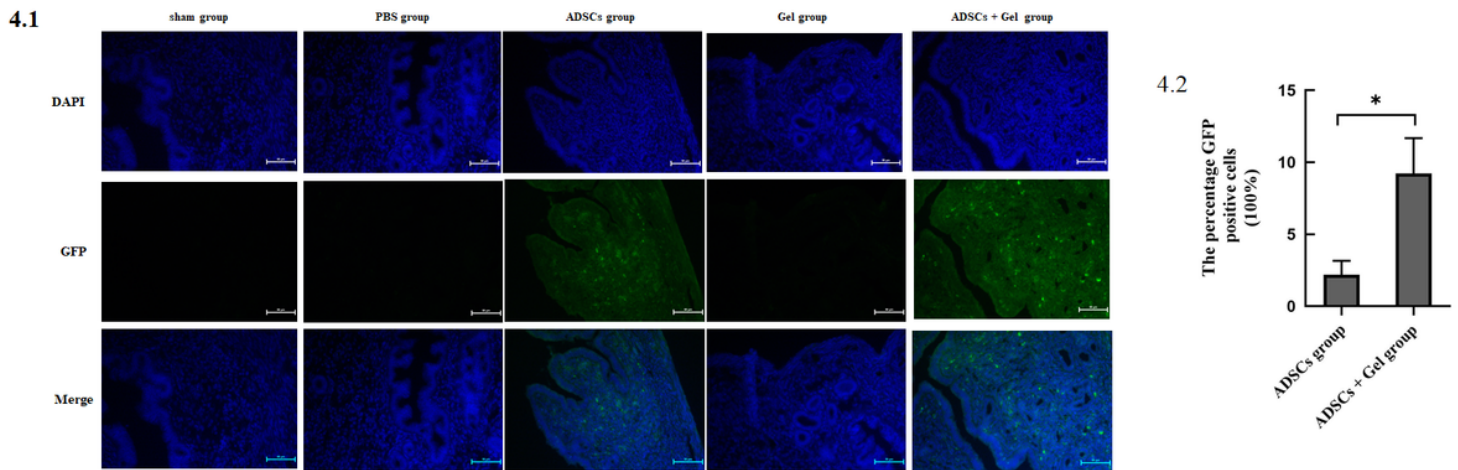


Figure 4

Engraftment of the endometrium with ADSCs following local injection. 4.1 Fluorescence microscopy analysis of uterine tissue sections (Scale bar=50μm). 4.2 The percentage GFP-positive cells of ADSCs + Gel group (9.215 ± 2.470%, n=3) was higher than ADSCs group (2.175 ± 0.9816%, n=3) (*P<0.05).

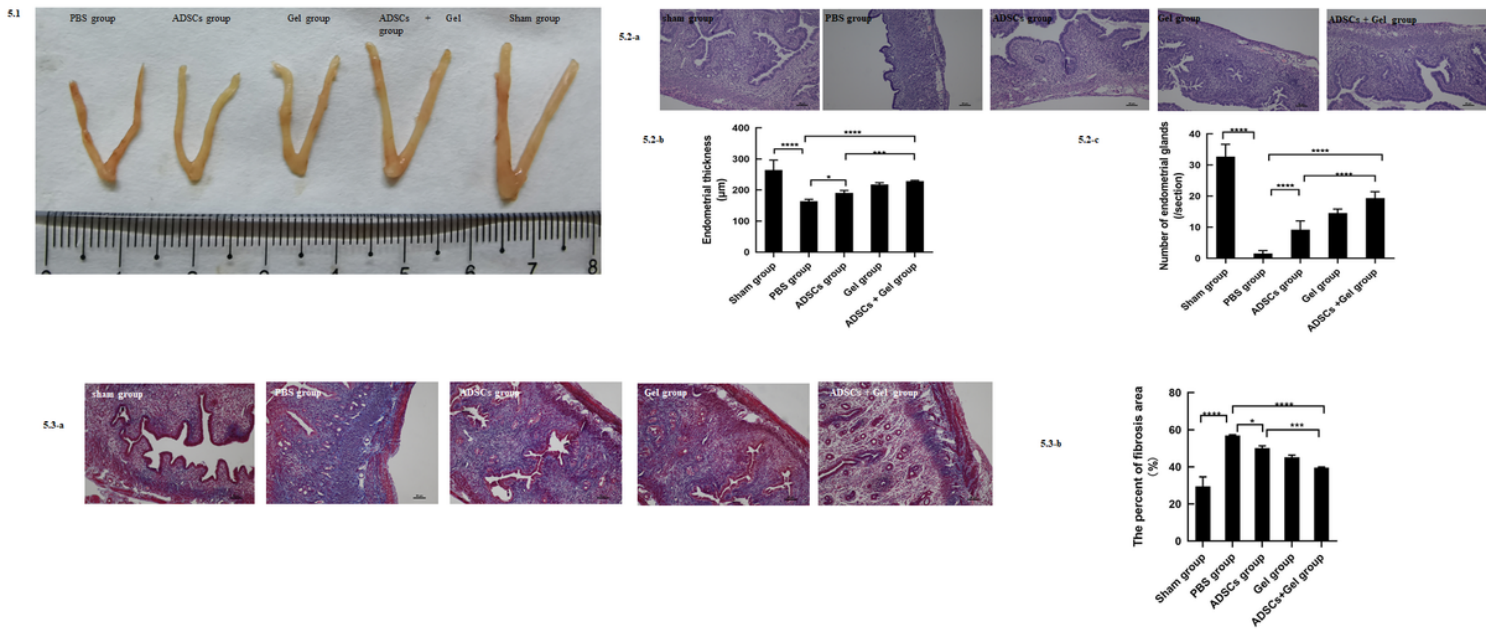


Figure 5

Uterine morphological features and changes. 5.1 The macroscopic appearance of the uterus. 5.2-a H&E staining of mice uterine tissue (Scale bar=50 µm). 5.2-b The endometrial thickness at transplantation day seven. Sham group, 264.5 ± 31.75 µm; PBS group, 163.8 ± 6.128 µm; ADSCs group, 190.1 ± 8.389µm; Gel group, 217.8 ± 5.839µm; ADSCs + Gel, 228.8 ± 2.254 µm. 5.2-c The number of endometrial glands at transplantation day seven. Sham group, 32.73 ± 3.952/section; PBS group, 1.545 ± 0.9342/section; ADSCs group, 9.182 ± 2.857/section; Gel group, 14.55 ± 1.293/section; ADSCs + Gel, 19.36 ± 2.063/section. *P < 0.05, **P < 0.01, ***P<0.001, ****P<0.0001. 5.3-a Masson staining of mice uterine tissue (Scale bar=50µm). 5.3-b The percent of fibrosis area at transplantation day seven. Sham group, 29.44 ± 5.2305%; PBS group, 56.89 ± 0.4425%; ADSCs group, 50.10 ± 1.280%; Gel group, 45.17 ± 1.196%; ADSCs + Gel, 39.55 ± 0.4125%. *P < 0.05, **P < 0.01, ***P<0.001, ****P<0.0001, ns P<0.05.

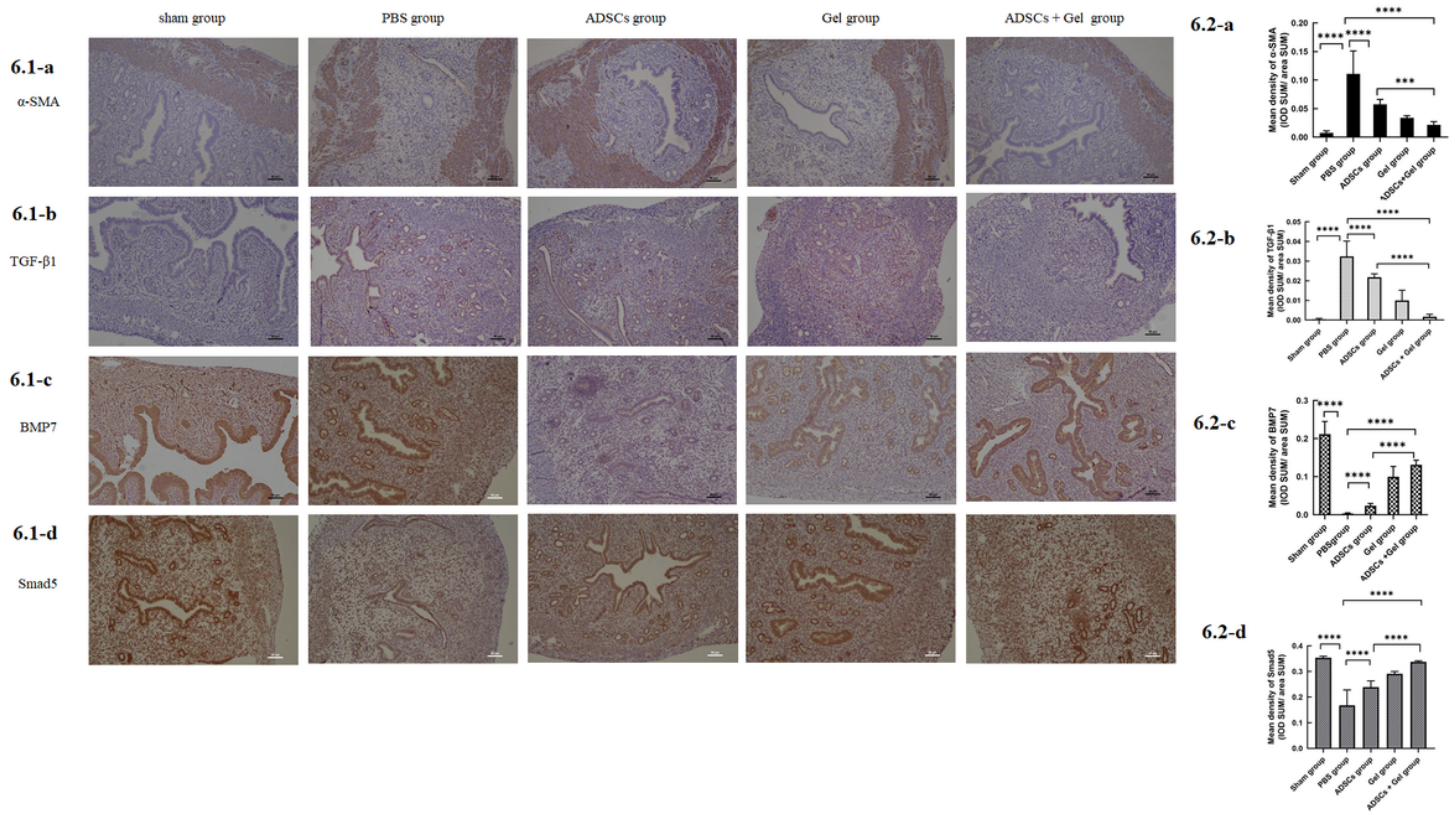
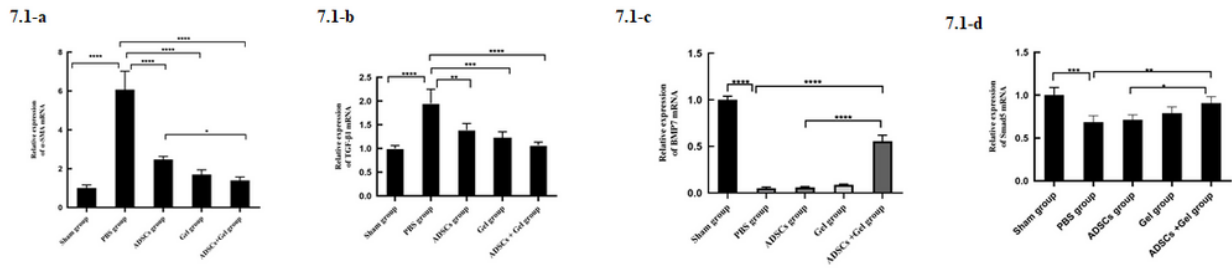
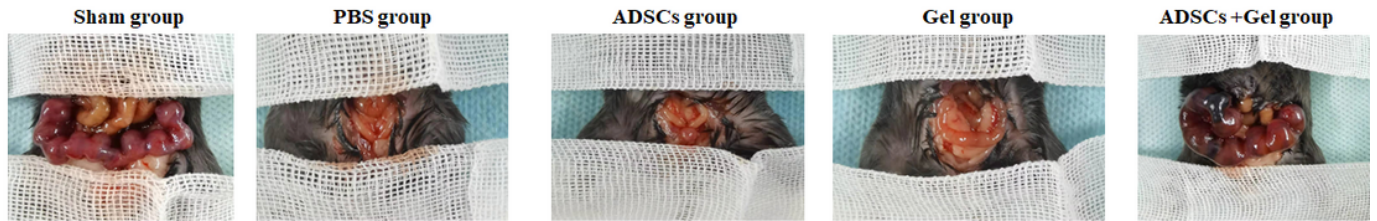


Figure 6

Immunohistochemistry results 6.1 Representative immunostaining of α-SMA, TGF-β1, BMP7 and Smad5 (Scale bar=50μm). 6.2-a Mean density of α-SMA, Sham group, 0.007813 ± 0.003258 ; PBS group, 0.1109 ± 0.04010 ; ADSCs group, 0.05746 ± 0.008630 ; Gel group, 0.03392 ± 0.003734 ; ADSCs + Gel, 0.02151 ± 0.005611 . 6.2-b Mean density of TGF-β1, Sham group, 0.0004134 ± 0.0004932 ; PBS group, 0.03246 ± 0.007779 ; ADSCs group, 0.02180 ± 0.001778 ; Gel group, 0.009999 ± 0.005183 ; ADSCs + Gel, 0.001736 ± 0.001229 . 6.2-c Sham group, 0.2119 ± 0.03328 ; PBS group, 0.002817 ± 0.002115 ; ADSCs group, 0.02330 ± 0.006284 ; Gel group, 0.09967 ± 0.02718 ; ADSCs + Gel, 0.1314 ± 0.01210 . 6.2-d Mean density of Smad5, Sham group, 0.3536 ± 0.005790 ; PBS group, 0.1676 ± 0.06002 ; ADSCs group, 0.2391 ± 0.02442 ; Gel group, 0.2910 ± 0.009053 ; ADSCs + Gel, 0.3372 ± 0.004266 . *P < 0.05, **P < 0.01, ***P < 0.001, ****P < 0.0001, ns P > 0.05.



7.2



N=5	Sham group	PBS group	ADSCs group	Gel group	ADSCs +Gel group
Mean number of fetuses	9	0	0	0	5

Figure 7

7.1-a Relative expression of α -SMA mRNA. Sham group, 1.008 \pm 0.1544; PBS group, 0.1544 \pm 0.9503; ADSCs group, 2.474 \pm 0.1598; Gel group, 1.703 \pm 0.2415; ADSCs + Gel, 1.398 \pm 0.1797. 7.1-b Relative expression of TGF- β 1 mRNA. Sham group, 1.001 \pm 0.05932; PBS group, 1.951 \pm 0.2980; ADSCs group, 1.391 \pm 0.1269; Gel group, 1.227 \pm 0.1269; ADSCs + Gel, 1.068 \pm 0.06639. 7.1-c Relative expression of BMP7 mRNA. Sham group, 1.001 \pm 0.03872; PBS group, 0.05062 \pm 0.01281; ADSCs group, 0.06124 \pm 0.006388; Gel group, 0.08836 \pm 0.005922; ADSCs + Gel, 0.5575 \pm 0.06289. 7.1-d Relative expression of Smad5 mRNA. Sham group, 1.003 \pm 0.08697; PBS group, 0.6843 \pm 0.07691; ADSCs group, 0.7127 \pm 0.05734; Gel group, 0.7891 \pm 0.07409; ADSCs + Gel, 0.9066 \pm 0.07593. *P < 0.05, **P < 0.01, ***P \leq 0.001, ****P \leq 0.0001, ns \geq 0.05. 7.2 The results of mating experiment.